### 1 The maize PLASTID TERMINAL OXIDASE (PTOX) locus controls the

2 carotenoid content of kernels.

3

- 4 Yongxin Nie<sup>1,11</sup>, Hui Wang<sup>2,11</sup>, Guan Zhang<sup>3,11</sup>, Haiping Ding<sup>1,11</sup>, Beibei Han<sup>3</sup>, Lei Liu<sup>4</sup>,
- 5 Jian Shi<sup>2</sup>, Jiyuan Du<sup>1</sup>, Xiaohu Li<sup>1</sup>, Xinzheng Li<sup>1</sup>, Yajie Zhao<sup>1</sup>, Xiaocong Zhang<sup>5</sup>,
- 6 Changlin Liu<sup>5</sup>, Jianfeng Weng<sup>5</sup>, Xinhai Li<sup>5</sup>, Xiansheng Zhang<sup>1</sup>, Xiangyu Zhao<sup>1</sup>,
- 7 Guangtang Pan<sup>2</sup>, David Jackson<sup>6</sup>, Qin-Bao Li<sup>7</sup>, Philip S Stinard<sup>8</sup>, Jennifer Arp<sup>9,10</sup>,
- 8 Martin M Sachs<sup>8,9</sup>, Steven Moose<sup>9</sup>, Charles T Hunter<sup>7</sup>, Qingyu Wu<sup>3\*</sup>, Zhiming Zhang<sup>1\*</sup>

9

- 10 <sup>1</sup>State Key Laboratory of Crop Biology, College of Life Sciences, Shandong
- 11 Agricultural University, Taian 271018, China;
- <sup>2</sup>Maize Research Institute, Sichuan Agricultural University, Chengdu 611130, China;
- <sup>3</sup>State Key Laboratory of Efficient Utilization of Arid and Semi-arid Arable Land in
- Northern China (the Institute of Agricultural Resources and Regional Planning, Chinese
- 15 Academy of Agricultural Sciences, Beijing 100081, China);
- <sup>4</sup>National Key Laboratory of Crop Genetic Improvement, Hubei Hongshan Laboratory,
- Huazhong Agricultural University, Wuhan 430070, China;
- <sup>5</sup>Institute of Crop Sciences, Chinese Academy of Agricultural Sciences, Beijing 100081,
- 19 China;
- <sup>6</sup>Cold Spring Harbor Laboratory, Cold Spring Harbor, New York 11724, USA;
- <sup>7</sup>USDA-ARS, Chemistry Research Unit, Gainesville, FL 32608;
- <sup>8</sup> USDA-ARS, Maize Genetics Cooperation Stock Center, Urbana, IL 61801;
- <sup>9</sup> University of Illinois at Urbana-Champaign, Department of Crop Sciences, Urbana,
- 24 IL 61801;
- 25 <sup>10</sup> Bayer Crop Science 700 Chesterfield Parkway West, Chesterfield, MO 63017, USA;
- 26 <sup>11</sup>These authors contributed equally.

27

- 28 \*To whom correspondence should be addressed, Zhiming Zhang, Email:
- 29 <u>zhzhang@sdau.edu.cn</u> or Qingyu Wu (ORCID: 0000-0003-3064-2445), Email:
- 30 wuqingyu@caas.cn

#### **SUMMARY**

Carotenoids perform a broad range of important functions in humans; therefore, carotenoid biofortification of maize ( $Zea\ mays\ L.$ ), one of the most highly produced cereal crops worldwide, would have a global impact on human health.  $PLASTID\ TERMINAL\ OXIDASE\ (PTOX)$  genes play an important role in carotenoid metabolism; however, the possible function of PTOX in carotenoid biosynthesis in maize has not yet been explored. In this study, we characterized the maize PTOX locus by forward- and reverse-genetic analyses. While most higher plant species possess a single copy of the PTOX gene, maize carries two tandemly duplicated copies. Characterization of mutants revealed that disruption of either copy resulted in a carotenoid-deficient phenotype. We identified mutations in the PTOX genes as being causal of the classic maize mutant, albescent1. Remarkably, overexpression of ZmPTOX1 significantly improved the content of carotenoids, especially  $\beta$ -carotene (provitamin A), which was increased by  $\sim$ 3-fold, in maize kernels. Overall, our study shows that maize PTOX locus plays an important role in carotenoid biosynthesis in maize kernels and suggests that fine-tuning the expression of this gene could improve the nutritional value of cereal grains.

# **Keywords:**

carotene, provitamin A, biofortification, albescent1

#### Introduction

The lack of certain micronutrients poses a serious threat to human health. This is particularly true in developing countries, where people predominantly subsist on cereal grains, which lack some important nutrients. For example, carotenoids, a group of yellow or red pigments with antioxidant activity, are essential for human health but are present at low levels in cereal grains. Therefore, carotenoid biofortification of major cereal crops used as food and feed worldwide would have a global impact on human health (Wurtzel *et al.*, 2012, Owens *et al.*, 2014).

In plants, carotenoids function as accessory pigments during light harvesting and structural components of the photosynthetic apparatus. They also serve a precursor for numerous secondary metabolites and plant hormones such as abscisic acid (ABA) and strigolactones (Nisar et al., 2015; Jia et al., 2018). The carotenoid metabolic pathway has been intensively studied in plants (reviewed by (Collini, 2019). Carotenoids are synthesized in plastids from the colorless pigment phytoene via a series of sequential desaturation reactions. The first two desaturation reactions are catalyzed by phytoene desaturase (PDS), which result in the formation of phytofluene and then ζ-carotene (Bartley et al., 1991). The  $\zeta$ -carotene is then catalyzed by  $\zeta$ -carotene desaturase (ZDS) to form neurosporene and then lycopene (Albrecht et al., 1995). Lycopene is cyclized to form either  $\alpha$ - or  $\beta$ -carotene, which can be oxidized to produce xanthophylls in photosynthetic tissues. PDS and ZDS require plastoquinone (PQ) as an electronaccepting cofactor (Norris et al., 1995) and PQ is maintained in an available (oxidized) state for these reactions by plastid terminal oxidase (PTOX) (Joet et al., 2002, Kuntz, 2004, Foudree et al., 2012). PTOX also serves to protect photosynthetic machinery during conditions of photo-oxidative stress (Cournac et al., 2002, Stepien and Johnson, 2018).

The first plant *PTOX* gene was identified in the *immutans* (*im*) mutant of *Arabidopsis thaliana* (Carol *et al.*, 1999, Wu *et al.*, 1999), which shows a variegated phenotype. Cells in green sectors of the *im* mutant possess normal-appearing chloroplasts, while cells in the white sectors lack carotenoid pigments and appear to be blocked at various stages of chloroplast biogenesis (Wetzel *et al.*, 1994, Aluru *et al.*, 2001, Yu *et al.*, 2007). Orthologous mutants of *PTOX* in tomato (*Solanum lycopersicum* L.), are termed *ghost* mutants and have similar variegation in addition to pale or white immature fruit due to the lack of photo-protective carotenoids (Barr *et al.*, 2004).

Besides its function in carotenoid biosynthesis, PTOX also regulates plant architecture by affecting the biosynthesis of plant hormones. Rice (*Oryza sativa* L.) *ptox* mutants show variegation similar to *im* and *ghost*, but also exhibit excessive tillering and semidwarfism, due to deficiency of strigolactones (Tamiru *et al.*, 2014). *Chlamydomonas reinhardtii* possesses two isoforms of PTOX with, one of which appears to have a greater role in regenerating PQ for use by PDS while the other functions primarily during photosynthesis (Houille-Vernes *et al.*, 2011).

Although the importance of *PTOX* genes for carotenoid metabolism, chloroplast function, and shoot architecture has been characterized in various plant species, the function of these genes in maize (*Zea mays* L.), the most produced cereal crop, has not yet been reported. Here, we identified the maize *PTOX* locus, containing two functional genes, by forward- and reverse-genetic approaches. Characterization of *Zmptox1* and *Zmptox2* mutants reveals an important role of the *PTOX* locus in carotenoid biosynthesis in maize leaves and kernels. We demonstrate that engineering this gene can enhance the carotenoid content and nutritional value of maize grains.

#### Results

# Map-based cloning of *ZmPTOX1*

To identify the key genes involved in carotenoid biosynthesis in maize kernels, we performed ethyl methanesulfonate (EMS) mutagenesis screening on the Chinese elite maize inbred line RP125 and searched for mutants with pale kernels, an indicator of low carotenoid accumulation in the endosperm (Nie *et al.*, 2021). A mutant with much paler kernels than the wild type (RP125, yellowish kernels) was identified in the M2 population (Figure 1a). The mutants also displayed leaf variegation, with white and green sectors, at the seedling stage (Figure 1b) and accumulated less chlorophyll than the wild-type plants (Figure 1c). Together, these results suggest that the mutants exhibit not only low carotenoid accumulation but also abnormal chloroplast biogenesis.

To identify and clone the causal gene, we generated a recombinant F2 population by crossing the recessive mutant with B73 inbred line and performed bulked segregant analysis (BSA) using pooled RNA samples representing approximately 30 mutant or wild-type kernels (Gallavotti and Whipple, 2015). We mapped the gene to an approximately 2 Mb region on the short arm of chromosome 2. Using  $\sim$ 850 individual mutants, we narrowed down the region to  $\sim$ 100 kb containing two putative genes in the B73 reference genome v4, Zm00001d001909 (hereafter ZmPTOXI) and

Zm00001d001908 (hereafter ZmPTOX2). Gene models indicate multiple transcript variants for both genes at this locus. The most recent gene models for B73 (Zm0001eb066920 from B73-REFERENCE-NAM-5.0 [B73v5]) has four transcript variants for ZmPTOX1 with variations in splicing of the third, fourth, and fifth exons. We sequenced full length cDNAs and confirmed the presence of two transcript variants for ZmPTOX1, matching T001 and T004 from Zm0001eb066920 (Figure 2 and Supplementary data 1). Gene models for ZmPTOX2 are more complex and appear to incorrectly include multiple independent genes in some cases. In B73v5 (Zm00001eb066910) there are two variants with differences restricted to the 3' end. Our sequencing of cDNAs of ZmPTOX2 provided evidence for two transcripts (T01 and T02) with 86.9% identify with ZmPTOX1 (Figure 2 and Supplementary data 1). Sequencing the *PTOX* locus of the EMS mutant revealed a G-to-A mutation in the exon 5 of Zm00001d001909, which was predicted to change the tryptophan residue at position 186 to a premature stop codon (Figure 1d). We also identified two additional mutants, with phenotypes like Zmptox1-1, in our EMS collection (Figure 1e and Supplementary Figure 1a). Both alleles carried mutations at splice sites in Zm00001d001909, leading to incorrectly spliced transcripts. The mutation on the splicing site of Zmptox1-2 introduced a 36-bp deletion within the transcript leading to a 12 AA deletion on the alternative oxidase (AOX) domain, which is critical to the biochemical function of PTOX (Supplementary figure 1b, c). The mutation on the splicing site of Zmptox1-3 caused a 128-bp intron retention and introduced a premature stop codon (Figure 1d and Supplementary Figure 1b, d). The F1 plants obtained by crossing these mutants displayed similar phenotypes (Figure 1e), confirming that the two mutants were allelic, and that the mutations in Zm00001d001909 were responsible for the pale phenotype of kernels. To further validate the association between disruption of ZmPTOX1 and the phenotype, we sought additional UniformMu Mutator transposon alleles of Zmptox1 from the Maize Genetics Cooperation Stock Center (Settles et al., 2007, McCarty et al., 2013). Three transposon insertions were identified in Zmptox1 (Figure 2). The

119

120

121

122

123

124

125

126

127

128

129

130

131

132

133

134

135

136

137

138

139

140

141

142

143

144

145

146

147

148

Zmptox1-umu1 (mu1034172) insertion occurred across the intron-exon border at the 5'

end of exon 2 and co-segregated with pale kernels that germinated into seedlings with pale leaves. These plants were able to grow to maturity and produced ears with uniformly pale kernels.

The classic maize mutant *albescent1* (*al1*) is characterized by pale kernels that germinate into seedling having pale or sectored leaves, and maps close by the *Zmptox* locus (Stinard, 2014). We obtained an allelic series of *al1* mutants and conducted Sanger sequencing of PCR-amplified *ZmPTOX1* and *ZmPTOX2* genomic DNA and cDNA from *al1* mutant seedlings to test association between the *al1* phenotype and *ZmPTOX* (Supplemental data 1). We found that *al1-gl2-ref*, *al1-y3*, *al1-y5*, and *al1-Sprague* all contained a 94-base tandem duplication of exon 7 in *ZmPTOX2* that would introduce a premature stop codon (Figure 2). These alleles all contained fulllength, intact transcripts for *ZmPTOX1*. The *al1-Brawn* mutant contained deletions in both *ZmPTOX1* (278 bp deletion that causes a -186 bp in-frame deletion within the mRNA leading to a 62 AA deletion) and *ZmPTOX2* (286 bp deletion that would disrupt the reading frame) (Figure 2). The fact that the leaf color varies between these alleles is likely due to the variable penetrance of these mutants in different genetic backgrounds.

# ZmPTOX1 regulates carotenoid biosynthesis in maize kernels

Protein BLAST and phylogenetic analysis revealed that *Zm00001d001909* encodes PTOX (Figure 3a), an enzyme that activates the plastid enzyme PDS, which in turn converts the colorless phytoene to ζ-carotene, a precursor of colored carotenoids ((Wetzel *et al.*, 1994) and Figure 3b). PTOX acts to maintain oxidized PQ to serve as a cofactor of PDS and ZDS, two enzymes required for carotenoid biosynthesis. To determine whether this mechanism is conserved in maize kernels, we examined the activities of PDS and ZDS in wild-type and *Zmptox1-1* kernels. Both enzymes showed reduced activity in mutant kernels compared with wild-type kernels (Figure 3c and d), suggesting that ZmPTOX1 participates in carotenoid biosynthesis by regulating the activity of PDS and ZDS via control of available PQ9.

To confirm whether the pale color of mutant kernels was indeed caused by the lower accumulation of colored carotenoids, we measured the contents of colored carotenoids, including lutein, zeaxanthin, and carotene, as well as that of phytoene in wild-type and mutant kernels. The mutant kernels accumulated more noncolored pigments such as phytoene (Figure 3e) and fewer colored pigments such as lutein and zeaxanthin (Figure 3f and g). Additionally, neither  $\alpha$ -carotene nor  $\beta$ -carotene was

detected in mutant kernels. These results confirmed that the pale color of mutant kernels resulted from impairment of carotenoid biosynthesis due to the disruption of *ZmPTOX1*.

To gain further insights into the transcriptomic changes in *Zmptox1* mutant kernels, we performed RNA-seq analyses on wild-type and Zmptox1-1 mutant kernels sampled at 9, 12, and 20 dpp. Principal component analysis (PCA) showed strong correlation among the biological replicates of each genotype, indicating that our RNA-seq data were highly reliable (Supplementary Figure 2a). Comparison between the RNA-seq data of Zmptox1 and wild-type kernels led to the detection of 1,523 (905 upregulated and 618 downregulated), 571 (283 upregulated and 288 downregulated), and 523 (277 upregulated and 246 downregulated) differentially expressed genes (DEGs) at 9, 12, and 20 dpp, respectively (Supplementary Table 1). A total of 26 DEGs were significantly upregulated, and 26 DEGs were downregulated, at least at one time point (Supplementary Figure 2b and c). Functional enrichment analysis of the DEGs using the Kyoto Encyclopedia of Genes and Genomes (KEGG) database revealed 20 representative pathways at three developmental stages (Figure 4a), among which the 'plant-pathogen interaction pathway' was the most highly enriched, suggesting that either PTOX functions in pathogen resistance or changes in carotenoid metabolism affect pathogen fitness. A closer look at the transcriptomes revealed that the expression of genes involved in methylerythritol phosphate (MEP), mevalonate (MVA), and carotenoid pathways remained largely unchanged in ptox1 mutant kernels compared with wild-type kernels (Figure 4b).

Phenotypes associated with the disruption of PTOX have been reported in other plant species such as Arabidopsis, tomato, and rice; however, these phenotypes were related only to changes in leaf color, fruit color, and shoot architecture and not to changes in seed color (Carol et al., 1999, Wu et al., 1999, Barr et al., 2004, Tamiru et al., 2014). Additionally, Arabidopsis, tomato, and rice possess only one copy of PTOX, whereas maize has two tandemly duplicated PTOX genes separated by  $\sim$ 80 kb (Figure 3a). ZmPTOXI transcripts were more abundant than ZmPTOX2 transcripts (Figure 4d), consistent with a previous study (Walley et al., 2016)), which could explain why the impairment of ZmPTOXI alone was sufficient to cause pale kernels and variegated leaves. Indeed, the expression of ZmPTOXI was unchanged in ZmptoxI mutants, not upregulated so-as to complement the ZmPTOXI deficiency (Figure 4c).

To determine whether natural variation in ZmPTOX1 is associated with carotenoid content, we conducted a candidate gene association study using a maize association

panel (n = 368 diverse inbred lines) and previously published carotenoid content data (Fu et al., 2013). The results revealed four single nucleotide polymorphisms (SNPs) and one InDel in ZmPTOX1, all of which showed significant association with carotenoid content. Three SNPs (2.2779620 T > C, 2.2779776 A > C, 2.2779998 A > G) were associated with  $\alpha$ -carotene content, while the remaining one SNP (2.2778989 C > T) and one InDel (2.2778979 TTTTC > T) in the promoter region of ZmPTOX1 were associated with the lutein content of kernels (Figure 5a). Among the three αcarotene content-associated SNPs, two were found in the intron and one in the exon (2,779,620 bp). The exonic SNP was nonsynonymous and predicted to cause prolineto-serine amino acid substitution. Consistent with our finding, ZmPTOX1 was also found to be associated with the carotenoid content of maize kernels in a separate GWAS study that was conducted using the US nested association mapping panel (Diepenbrock et al., 2021). Overall, our findings showed that natural variation in ZmPTOX1 influences lutein and  $\alpha$ -carotene contents (Figure 5b, c and Supplemental Table 3), suggesting that the manipulation of this gene may enhance the carotenoid content of maize kernels.

A previous study showed that maize represents, on average, only 57.1% of the nucleotide diversity in teosinte (Wright *et al.*, 2005). To determine whether ZmPTOXI underwent selection during maize domestication and improvement, we calculated the nucleotide diversity of ZmPTOXI in improved maize lines, landraces, and teosinte using HapMap 3 (Bukowski *et al.*, 2017). Nucleotide diversity was high in teosinte but significantly reduced in the improved maize lines, especially in the region highlighted in red in Figure 5d ( $\pi_{Maize}/\pi_{Teosinte} = 15\%$ ). Furthermore, coalescent simulations incorporated the demographic history of maize domestication and  $\pi_{Teosinte}/\pi_{Maize} > 2.98$  (P < 0.01) showed a significant deviation from the neutral expectation. These data suggest that ZmPTOXI underwent positive selection throughout the maize domestication process; however, the implication of this selection remains to be explored.

### Overexpression of ZmPTOX1 improves nutritional content of maize kernels

To determine whether *ZmPTOX1* could directly enhance the nutritional content of maize kernels, we overexpressed *ZmPTOX1* under the control of the maize ubiquitin promoter. Ten independent events were obtained, three of which were randomly selected for further analysis. Quantitative real-time PCR (qRT-PCR) revealed that

ZmPTOXI was upregulated 10–45-fold in all three overexpression (OE) lines relative to the wild-type controls (Figure 6a). Additionally, the levels of lutein, zeaxanthin, and  $\alpha$ -carotene were nearly 2-fold greater, and the levels of the  $\beta$ -carotene were 3-fold higher, in transgenic kernels than in wild-type controls (Figure 6b–e). We also examined the activities of PDS and ZDS in B104 and OE-2. Both enzymes showed slightly increased activity in OE line (Supplementary Figure 3a, b). However, we did not observe a significant increase of ZmPSYI expression in OE lines (Supplementary Figure 3c), suggesting that ZmPTOX does not regulate PSYI at the transcriptional level. These findings demonstrate that manipulating ZmPTOXI expression is effective in improving maize carotenoid content.

### **DISCUSSION**

Through forward genetic screening, we identified a PTOX gene in maize, one of the most important cereal crops worldwide, and demonstrated that engineering this gene dramatically increases the levels of carotenoids, particularly  $\beta$ -carotene, a nutrient crucial for human health. The carotenoid biosynthetic pathway in plants has been established through the cloning and characterization of genes using specific carotenoid mutants. Although phytoene synthase (PSY), which is responsible for phytoene biosynthesis, has received much attention as a rate-limiting enzyme in this pathway (Zhou  $et\ al.$ , 2015, Chayut  $et\ al.$ , 2017), the PDS and ZDS enzymes, which desaturate phytoene and  $\zeta$ -carotene, are also critical for the biosynthesis of downstream health-promoting carotenoids (McQuinn  $et\ al.$ , 2018). Thus, new bottlenecks emerge in subsequent desaturation steps to promote the activity of PDS and ZDS. Our data show that PTOX is a promising target for engineering maize cultivars with high carotenoid content.

Although the maize genome carries two tandemly duplicated *PTOX* genes, in contrast to the single *PTOX* gene in *Arabidopsis*, tomato, and rice, disrupting one of the two copies in maize is sufficient to impair carotenoid biosynthesis in grains. *PTOX* exists as a single-copy gene in most plant species (Carol *et al.*, 1999, Wu *et al.*, 1999, Barr *et al.*, 2004, Tamiru *et al.*, 2014); however, in some cyanobacteria and algae, two copies of the *PTOX* gene have been reported (Wang *et al.*, 2009, Houille-Vernes *et al.*, 2011), of which one copy is more important than the other. For example, *Chlamydomonas* has *PTOX1* and *PTOX2*; however, PTOX2 is the predominant enzyme

isoform involved in chlororespiration, and the *ptox2* single mutant shows lower fitness than the wild type when grown under phototrophic conditions (Houille-Vernes *et al.*, 2011). Our study is the first describing a higher plant containing two copies of *PTOX*, and that disrupting one copy is sufficient to cause obvious phenotypes. Although both *ZmPTOX1* and *ZmPTOX2* were expressed in a variety of tissues, *ZmPTOX1* transcripts were more abundant than *ZmPTOX2* transcripts in the majority of maize tissues (Figure 4d and (Walley *et al.*, 2016)), particularly mature leaves and endosperm, which showed clear changes in color because of decreased pigment accumulation (Figure 1a,c; Figure 2h). Our findings imply that *ZmPTOX1* plays a major role in carotenoid biosynthesis, and its disruption is sufficient to impair this process. However, whether the maize *PTOX* genes exhibit a dosage effect remains to be explored. Elevating the abundance of *ZmPTOX1* transcripts increased downstream carotenoid abundance, indicating that dosage effect is likely (Figure 5). However, detailed characterization of *Zmptox1* and *Zmptox2* single and double mutants in the same genetic background is required before drawing firm conclusions.

In addition to chloroplast biogenesis and carotenoid biosynthesis, PTOXs are also potentially involved in other physiological processes such as stress tolerance and plant development (Tamiru et al., 2014, Johnson and Stepien, 2016). For example, transgenic tobacco plants transformed with the PTOX1 gene of the green alga Chlamydomonas reinhardtii outperformed wild-type controls in terms of seed germination rate, root length, and shoot biomass accumulation under high NaCl concentrations. Transgenic tobacco plants also displayed better recovery and less chlorophyll bleaching than wildtype plants after the NaCl treatment (Ahmad et al., 2020). Rice ptox mutants displayed excessive tillering and a semidwarf phenotype, demonstrating the importance of PTOX in strigolactone biosynthesis (Tamiru et al., 2014). However, the Zmptox1 mutants did not exhibit obvious developmental phenotypes compared with wild-type plants. One explanation is that the two ZmPTOX genes in maize perform redundant functions; thus, ZmPTOX2 can compensate for the loss of function of ZmPTOX1 and is adequate to sustain the biosynthesis of strigolactones in the Zmptox1 mutant. To verify whether ZmPTOX1 and ZmPTOX2 are redundant genes, double mutants are needed. Given the diverse functions of PTOXs in regulating carotenoid biosynthesis, plant development,

and stress resistance, fine-tuning the expression of *ZmPTOX1* has potential to both improve the nutritional value and enhance the stress tolerance of maize.

### **Experimental Procedures**

### Identification and map-based cloning of the ZmPTOX1 gene

To identify the *PTOX* gene in maize, pollen (2 ml) of the RP125 inbred line (wild type) were treated with 0.066% EMS (Sigma-Aldrich, M0880) solution in mineral oil (Sigma-Aldrich, M8410) for 30 min. The mutagenized pollen was then used to pollinate the ears of RP125. The F2 segregating population was constructed by crossing the M2 *Zmptox1* mutants in the RP125 background with B73. RNA was extracted from ~30 pooled normal or mutant seeds, and BSA-seq was performed as described previously (Gallavotti and Whipple, 2015). Candidate genes in the mapping region were amplified from the mutants and subjected to Sanger sequencing. The deduced amino acid sequences of these candidate genes were aligned using the MUSCLE model, and a phylogenetic tree was constructed using the neighbor-joining method in MEGA7 with 1,000 bootstrap replicates (Kumar *et al.*, 2016).

The UniformMu alleles in *ZmPTOX1*, mu1034172 (*ptox1-umu1*) in UFMu-03227,

The UniformMu alleles in *ZmPTOX1*, mu1034172 (*ptox1-umu1*) in UFMu-03227, and the classic *albescent1* (*al1*) alleles, *al1-gl2-ref*, *al1-Brawn*, *al1-y3*, *al1-Sprague*, and *al1-1998*, were obtained from the Maize Genetic Cooperation Stock Center. The UniformMu families were analyzed for the presence of the transposons in *ZmPTOX1* by PCR using gene-specific primers along with a *Mutator*-specific terminal inverted repeat primer TIR6 Mutant leaf samples from the *al1* alleles were sampled for genomic DNA and RNA. cDNA was made using the SuperScript IV First-Strand Synthesis System (Invitrogen, Cat. 18091050). Transcript specific primers were used to amplify cDNAs from normal and mutant leaf samples to identify transcript variants and possible causal mutations. Genomic and cDNA sequences were amplified using gene-specific primers and sequenced using Sanger sequencing. Conditions for all PCR reactions followed protocols from Phusion high-fidelity DNA polymerase (NEB, Cat. M0530L). See Supplemental Table 2 for primer sequences.

#### **Overexpression Lines**

The *ZmPTOX1* overexpression vector was constructed by cloning the coding region of *ZmPTOX1* under the control of the maize ubiquitin promoter. The construct was transformed into *Agrobacterium*, which was then used to transform the maize inbred line B104 as described previously (Frame *et al.*, 2015).

#### Carotenoid analysis

The carotenoid extraction method described for alfalfa (Medicago truncatula) (Meng et al., 2019) was used in this study, with minor modifications. Seeds of the following genotypes were used for carotenoid extraction: wild type, Zmptox1-1, Zmptox1-2, Zmptox1-3, B104, and OE lines. Briefly, the dissected maize tissues (30 mg) were ground into powder in liquid nitrogen. Then, 200 µL of 6% (w/v) KOH (in methanol) was added to the ground tissue. The samples were vortexed for 10 s and heated at 60°C for 1 h in the dark. Subsequently, 200 µL of 50 mM HCl buffer (pH 7.5, containing 1 M NaCl) was added to each sample. Samples were allowed to cool to room temperature in the dark, thoroughly mixed by turning the tubes upside-down eight to ten times, and then incubated on ice for 10 min. Then, 800 µL of chloroform was added to the sample, mixed by inverting eight to ten times, and incubated on ice for 10 min. The mixtures were centrifuged at  $3,000 \times g$  for 5 min at 4°C. Then, the lower liquid phase (600 µL) was removed and again extracted using 800 µL of chloroform. The two chloroform extracts were combined, dried with a blowing device using high quality nitrogen, and then dissolved in 100 mL of ethyl acetate. The different pigments were identified by high performance liquid chromatography (HPLC; A30).

HPLC analysis was performed on seed as described previously (Fraser *et al.*, 2000), with minor modifications. Briefly, a C30 column at  $30 \pm 1^{\circ}$ C was used with solvent A (methanol, methyl cyanide, water, and butylated hydroxytoluene) and solvent B (methyl tert-butyl ether) as mobile phases, with a flow rate of 1.0 mL/min flow rate and an injection volume of 10  $\mu$ L. Carotenoids were identified by comparing their absorption spectra and retention period with those of the standards. The contents of carotenoids were calculated using standards.

The activities of PDS, ZDS, and PSY enzymes were determined using the ELISA-based method (LMAI Bio), according to the manufacturer's instructions. Solid-phase plant purified anti-PDS, -ZDS, and -PSY antibodies were used to coat microtiter plate wells. Then, PDS, ZDS, and PSY enzymes were added to the wells. An antibody–antigen–enzyme–antibody complex was labeled with combined antibodies and horse radish peroxidase (HRP). After thorough washing, the reaction was stopped by adding

sulfuric acid, which turns the TMB substrate blue when catalyzed by HRP. The color change was then measured spectrophotometrically at a wavelength of 450 nm. The optical density (OD) of the samples was then compared with the standard curve to determine the PDS, ZDS, and PSY concentrations in the samples.

### RNA-seq and data analysis

Kernels of wild-type and Zmptox1 mutant plants were harvested at 9, 12, and 20 days postpollination (dpp), with three biological replicates at each time point. Total RNA was extracted from the kernels using the TRIzol reagent, as directed by the manufacturer. The sequencing libraries were produced with the Illumina TruSeq RNA Sample Prep Kit and sequenced on the Illumina HiSeq X Ten System. The quality of raw sequence reads was checked using Fastp v.0.12.4 (Chen *et al.*, 2018). HISAT2 v.2.2.1, with default settings, was used to map the clean reads to the maize B73 RefGen\_V4 reference genome sequence (Kim *et al.*, 2015). StringTie v.2.0.4 was utilized to calculate gene expression levels as fragments per kilobase of transcript per million reads (FPKM) (Pertea *et al.*, 2016). DEGs were identified using DESeq2 based on two criteria: log2fold-change  $\geq 1$  and adjusted *p*-value cutoff  $\leq 0.05$  (Love *et al.*, 2014).

# Candidate gene association and nucleotide diversity analyses

Candidate gene association analysis was conducted using a maize association panel of 368 diverse inbred lines. *ZmPTOX1*-specific SNPs and InDels were downloaded from previous sequence data (Gui *et al.*, 2022) and metabolite content data of the members of this panel were downloaded from the previously released genotype dataset (Fu *et al.*, 2013). Association between metabolite contents and *ZmPTOX1*-specific SNPs and InDels (MAF > 0.05) was determined using a mixed linear model, after correction for familial relatedness and population structure, with a *p*-value of 0.001 as a threshold (Il Je *et al.*, 2018). The third-generation haplotype map data of *Zea mays* were downloaded. Nucleotide diversity was investigated in improved maize lines, landraces, and teosinte using vcftools (<a href="https://vcftools.github.io/examples.html">https://vcftools.github.io/examples.html</a>), with a 1 kb window and 100 bp step along the 2 kb upstream and 1 kb downstream regions of *ZmPTOX1*, respectively. coalescent simulations following the demographic history of maize domestication were performed using Ms program, with parameters as previously described, and running 10,000 coalescent simulations (Tian *et al.*, 2009, Huang *et al.*, 2018).

### 409 410 Acknowledgements 411 Funding for this work was provided by the National Natural Science Foundation of 412 China (32171925, U21A20210) to Q.W.; The National Key Research and Development 413 Program of China (2022YFD1201703), Taishan Scholars Program of Shandong 414 Province (tsqn201909074), and Shandong Natural Science Foundation (ZR2020KC019) 415 to Z.Z.; The Agricultural Science and Technology Innovation Program (GJ2023-14-11 416 417 and GJ2023-14-5) and Fundamental Research Funds for Central Non-profit Scientific Institution (G2023-01-30) to Q.W.; Key R&D Program of Shandong Province 418 (2021LZGC022-2) to H.D..; Shandong Natural Science Foundation (ZR2022MC076) 419 to Y.N.; National Science Foundation (NSF) to DJ (IOS-2129189); and United States 420 Department of Agriculture, Agricultural Research Service research project 6036-421 21000-011-00D to C.H. USDA is an equal opportunity provider and employer. We 422 thank Prof. Junjie Fu and Dr. Jie Zhang for their advice on nucleotide diversity analyses. 423 424 **Author contributions** 425 Q.W., Z.Z., Y.N., H.W., G.Z., H.D, D.J, G.P, X.Y.Z., X.S.Z., J.A., S.M., C.H., and 426 X.H.L. designed research and wrote the paper. Y.N., H.W., G.Z., and H.D. cloned the 427 ZmPTOX1 gene. J.S., J.D., X.L., X.Z.L., Y.Z., X.Z, C.L., J.W., G.PZ.Q., K.Z., Q.L., 428 Y.C., C.Z., C.L., J.W., X.L., X.S.Z., X.Y.Z, G.P., B.H, Q.L, J.A, M.S, S.M., C.H. L.L. 429 and D.J. performed candidate gene association analysis. 430 431 432 **Competing interests** The authors declare no competing interest. 433 434 Data availability 435 The raw data are available from Zhiming Zhang or Qingyu Wu upon request. All 436 RNAseq datasets reported in this study have been deposited in GenBank (NCBI) with 437 438 the following accession code: PRJNA943556. 439

440

- 442 **References**
- Ahmad, N., Khan, M.O., Islam, E., Wei, Z.Y., McAusland, L., Lawson, T., Johnson,
   G.N. and Nixon, P.J. (2020) Contrasting Responses to Stress Displayed by
   Tobacco Overexpressing an Algal Plastid Terminal Oxidase in the Chloroplast.
   Frontiers in Plant Science, 11.
- Albrecht, M., Klein, A., Hugueney, P., Sandmann, G. and Kuntz, M. (1995)
  Molecular-Cloning and Functional Expression in Escherichia-Coli of a Novel
  Plant Enzyme Mediating Zeta-Carotene Desaturation. *Febs Letters*, **372**, 199202.
- Aluru, M.R., Bae, H., Wu, D.Y. and Rodermel, S.R. (2001) The Arabidopsis immutans mutation affects plastid differentiation and the morphogenesis of white and green sectors in variegated plants. *Plant Physiology*, **127**, 67-77.
- Barr, J., White, W.S., Chen, L., Bae, H. and Rodermel, S. (2004) The GHOST terminal oxidase regulates developmental programming in tomato fruit. *Plant Cell and Environment*, 27, 840-852.
- Bartley, G.E., Viitanen, P.V., Pecker, I., Chamovitz, D., Hirschberg, J. and Scolnik,
  P.A. (1991) Molecular cloning and expression in photosynthetic bacteria of a
  soybean cDNA coding for phytoene desaturase, an enzyme of the carotenoid
  biosynthesis pathway. *Proceedings of the National Academy of Sciences, USA*,
  88, 6532-6536.
- Bukowski, R., Guo, X.S., Lu, Y.L., Zou, C., He, B., Rong, Z.Q., Wang, B., Xu, D.W.,
  Yang, B.C., Xie, C.X., Fan, L.J., Gao, S.B., Xu, X., Zhang, G.Y., Li, Y.R.,
  Jiao, Y.P., Doebley, J.F., Ross-Ibarra, J., Lorant, A., Buffalo, V., Romay,
  M.C., Buckler, E.S., Ware, D., Lai, J.S., Sun, Q. and Xu, Y.B. (2017)
  Construction of the third-generation Zea mays haplotype map. Gigascience, 7.
- Carol, P., Stevenson, D., Bisanz, C., Breitenbach, J., Sandmann, G., Mache, R.,
  Coupland, G. and Kuntz, M. (1999) Mutations in the Arabidopsis gene
  immutans cause a variegated phenotype by inactivating a chloroplast terminal
  oxidase associated with phytoene desaturation. *Plant Cell*, 11, 57-68.
- Chayut, N., Yuan, H., Ohali, S., Meir, A., Sa'ar, U., Tzuri, G., Zheng, Y., Mazourek,
   M., Gepstein, S., Zhou, X.J., Portnoy, V., Lewinsohn, E., Schaffer, A.A.,
   Katzir, N., Fei, Z.J., Welsch, R., Li, L., Burger, J. and Tadmor, Y. (2017)
   Distinct Mechanisms of the ORANGE Protein in Controlling Carotenoid Flux.
   Plant Physiology, 173, 376-389.
- Chen, S., Zhou, Y., Chen, Y. and Gu, J. (2018) fastp: an ultra-fast all-in-one FASTQ
   preprocessor. *Bioinformatics*, 34, i884-i890.
- Collini, E. (2019) Carotenoids in Photosynthesis: The Revenge of the "Accessory" Pigments. *Chem*, **5**, 494-495.
- Cournac, L., Latouche, G., Cerovic, Z., Redding, K., Ravenel, J. and Peltier, G. (2002) In vivo interactions between photosynthesis, mitorespiration, and chlororespiration in Chlamydomonas reinhardtii. *Plant Physiol*, **129**, 1921-1928.
- Diepenbrock, C.H., Ilut, D.C., Magallanes-Lundback, M., Kandianis, C.B., Lipka, A.E., Bradbury, P.J., Holland, J.B., Hamilton, J.P., Wooldridge, E.,

- Vaillancourt, B., E, G.N.-C., Wallace, J.G., Cepela, J., Mateos-Hernandez,
  M., Owens, B.F., Tiede, T., Buckler, E.S., Rocheford, T., Buell, C.R., Gore,
  M.A. and DellaPenna, D. (2021) Eleven biosynthetic genes explain the
  majority of natural variation in carotenoid levels in maize grain. *Plant Cell*, 33,
  882-900.
- Foudree, A., Putarjunan, A., Kambakam, S., Nolan, T., Fussell, J., Pogorelko, G. and Rodermel, S. (2012) The mechanism of variegation in immutans provides insight into chloroplast biogenesis. *Frontiers in Plant Science*, 3.
- Frame, B., Warnberg, K., Main, M. and Wang, K. (2015) Maize (Zea mays L.). In

  Agrobacterium Protocols. Methods in Molecular Biology (Wang, K. ed. New

  York, NY: Springer, pp. 101-117.

499

500

506

- Fraser, P.D., Pinto, M.E., Holloway, D.E. and Bramley, P.M. (2000) Technical advance: application of high-performance liquid chromatography with photodiode array detection to the metabolic profiling of plant isoprenoids. *Plant J*, **24**, 551-558.
- Fu, J.J., Cheng, Y.B., Linghu, J.J., Yang, X.H., Kang, L., Zhang, Z.X., Zhang, J.,
  He, C., Du, X.M., Peng, Z.Y., Wang, B., Zhai, L.H., Dai, C.M., Xu, J.B.,
  Wang, W.D., Li, X.R., Zheng, J., Chen, L., Luo, L.H., Liu, J.J., Qian, X.J.,
  Yan, J.B., Wang, J. and Wang, G.Y. (2013) RNA sequencing reveals the
  complex regulatory network in the maize kernel. *Nature Communications*, 4.
  - **Gallavotti, A. and Whipple, C.J.** (2015) Positional Cloning in Maize (Zea Mays Subsp Mays, Poaceae). *Applications in Plant Sciences*, **3**.
- Gui, S., Wei, W., Jiang, C., Luo, J., Chen, L., Wu, S., Li, W., Wang, Y., Li, S., Yang,
   N., Li, Q., Fernie, A.R. and Yan, J. (2022) A pan-Zea genome map for enhancing maize improvement. *Genome Biol*, 23, 178.
- Houille-Vernes, L., Rappaport, F., Wollman, F.A., Alric, J. and Johnson, X. (2011)
  Plastid terminal oxidase 2 (PTOX2) is the major oxidase involved in
  chlororespiration in Chlamydomonas. *Proceedings of the National Academy of*Sciences of the United States of America, **108**, 20820-20825.
- Huang, C., Sun, H., Xu, D., Chen, Q., Liang, Y., Wang, X., Xu, G., Tian, J., Wang,
  C., Li, D., Wu, L., Yang, X., Jin, W., Doebley, J.F. and Tian, F. (2018)
  ZmCCT9 enhances maize adaptation to higher latitudes. *Proc Natl Acad Sci U*SA, 115, E334-E341.
- Il Je, B., Xu, F., Wu, Q.Y., Liu, L., Meeley, R., Gallagher, J.P., Corcilius, L., Payne,
  R.J., Bartlett, M.E. and Jackson, D. (2018) The CLAVATA receptor
  FASCIATED EAR2 responds to distinct CLE peptides by signaling through two
  downstream effectors. *Elife*, 7.
- Joet, T., Genty, B., Josse, E.M., Kuntz, M., Cournac, L. and Peltier, G. (2002)
  Involvement of a plastid terminal oxidase in plastoquinone oxidation as
  evidenced by expression of the Arabidopsis thaliana enzyme in tobacco. *J Biol Chem*, 277, 31623-31630.
- Johnson, G.N. and Stepien, P. (2016) Plastid Terminal Oxidase as a Route to Improving Plant Stress Tolerance: Known Knowns and Known Unknowns. Plant and Cell Physiology, 57, 1387-1396.

- Kim, D., Langmead, B. and Salzberg, S.L. (2015) HISAT: a fast spliced aligner with low memory requirements. *Nat Methods*, **12**, 357-360.
- Kumar, S., Stecher, G. and Tamura, K. (2016) MEGA7: Molecular Evolutionary
  Genetics Analysis Version 7.0 for Bigger Datasets. *Molecular Biology and*Evolution, 33, 1870-1874.
- Kuntz, M. (2004) Plastid terminal oxidase and its biological significance. *Planta*, **218**, 896-899.
- Love, M.I., Huber, W. and Anders, S. (2014) Moderated estimation of fold change and dispersion for RNA-seq data with DESeq2. *Genome Biol*, **15**, 550.
- McCarty, D.R., Latshaw, S., Wu, S., Suzuki, M., Hunter, C.T., Avigne, W.T. and Koch, K.E. (2013) Mu-seq: sequence-based mapping and identification of transposon induced mutations. *PLoS One*, **8**, e77172.

543

544

- **McQuinn, R.P., Wong, B. and Giovannoni, J.J.** (2018) AtPDS overexpression in tomato: exposing unique patterns of carotenoid self-regulation and an alternative strategy for the enhancement of fruit carotenoid content. *Plant Biotechnology Journal*, **16**, 482-494.
- Meng, Y., Wang, Z., Wang, Y., Wang, C., Zhu, B., Liu, H., Ji, W., Wen, J., Chu, C.,
  Tadege, M., Niu, L. and Lin, H. (2019) The MYB Activator WHITE PETAL1
  Associates with MtTT8 and MtWD40-1 to Regulate Carotenoid-Derived
  Flower Pigmentation in Medicago truncatula. *Plant Cell*, **31**, 2751-2767.
- Nie, S.J., Wang, B., Ding, H.P., Lin, H.J., Zhang, L., Li, Q.G., Wang, Y.J., Zhang, 550 B., Liang, A.P., Zheng, Q., Wang, H., Lv, H.Y., Zhu, K., Jia, M.H., Wang, 551 X.T., Du, J.Y., Zhao, R.T., Jiang, Z.Z., Xia, C.N., Qiao, Z.H., Li, X.H., Liu, 552 B.Y., Zhu, H.B., An, R., Li, Y.C., Jiang, Q., Chen, B.F., Zhang, H.K., Wang, 553 D.N., Tang, C.X., Yuan, Y., Dai, J., Zhan, J., He, W.Q., Wang, X.B., Shi, J., 554 Wang, B., Gong, M., He, X.J., Li, P., Huang, L., Li, H., Pan, C., Huang, H., 555 Yuan, G.S., Lan, H., Nie, Y.X., Li, X.Z., Zhao, X.Y., Zhang, X.S., Pan, G.T., 556 Wu, Q.Y., Xu, F. and Zhang, Z.M. (2021) Genome assembly of the Chinese 557 maize elite inbred line RP125 and its EMS mutant collection provide new 558 resources for maize genetics research and crop improvement. Plant J, 108, 40-559 54. 560
- Norris, S.R., Barrette, T.R. and DellaPenna, D. (1995) Genetic dissection of carotenoid synthesis in arabidopsis defines plastoquinone as an essential component of phytoene desaturation. *Plant Cell*, **7**, 2139-2149.
- Owens, B.F., Lipka, A.E., Magallanes-Lundback, M., Tiede, T., Diepenbrock, C.H., Kandianis, C.B., Kim, E., Cepela, J., Mateos-Hernandez, M., Buell, C.R., Buckler, E.S., DellaPenna, D., Gore, M.A. and Rocheford, T. (2014) A Foundation for Provitamin A Biofortification of Maize: Genome-Wide Association and Genomic Prediction Models of Carotenoid Levels. *Genetics*, 198, 1699-+.
- Pertea, M., Kim, D., Pertea, G.M., Leek, J.T. and Salzberg, S.L. (2016) Transcriptlevel expression analysis of RNA-seq experiments with HISAT, StringTie and Ballgown. *Nat Protoc*, **11**, 1650-1667.
- 573 Settles, A.M., Holding, D.R., Tan, B.C., Latshaw, S.P., Liu, J., Suzuki, M., Li, L.,

- O'Brien, B.A., Fajardo, D.S., Wroclawska, E., Tseung, C.W., Lai, J., Hunter, C.T., 3rd, Avigne, W.T., Baier, J., Messing, J., Hannah, L.C., Koch, K.E., Becraft, P.W., Larkins, B.A. and McCarty, D.R. (2007) Sequence-indexed mutations in maize using the UniformMu transposon-tagging population. *BMC Genomics*, **8**, 116.
- 579 **Stepien, P. and Johnson, G.N.** (2018) Plastid terminal oxidase requires translocation 580 to the grana stacks to act as a sink for electron transport. *Proc Natl Acad Sci U* 581 *S A*, **115**, 9634-9639.
- 582 **Stinard, P.** (2014) A dominant enhancer of yellow color in albescent1 mutant 583 endosperms identified in South American orange flint lines. *Maize Genetics* 584 *Cooperation Newsletter*, **88**, 17.
- Tamiru, M., Abe, A., Utsushi, H., Yoshida, K., Takagi, H., Fujisaki, K., Undan, J.R.,
   Rakshit, S., Takaichi, S., Jikumaru, Y., Yokota, T., Terry, M.J. and Terauchi,
   R. (2014) The tillering phenotype of the rice plastid terminal oxidase (PTOX)
   loss-of-function mutant is associated with strigolactone deficiency. New
   Phytologist, 202, 116-131.
- Tian, F., Stevens, N.M. and Buckler, E.S.t. (2009) Tracking footprints of maize domestication and evidence for a massive selective sweep on chromosome 10.
   Proc Natl Acad Sci U S A, 106 Suppl 1, 9979-9986.
- Walley, J.W., Sartor, R.C., Shen, Z.X., Schmitz, R.J., Wu, K.J., Urich, M.A., Nery,
   J.R., Smith, L.G., Schnable, J.C., Ecker, J.R. and Briggs, S.P. (2016)
   Integration of omic networks in a developmental atlas of maize. Science, 353,
   814-818.
- Wang, J.X., Sommerfeld, M. and Hu, Q. (2009) Occurrence and environmental stress responses of two plastid terminal oxidases in Haematococcus pluvialis (Chlorophyceae). *Planta*, **230**, 191-203.
- Wetzel, C., Jiang, C., Meehan, L., Voytas, D.F. and Rodermel, S. (1994) Nuclear—organelle interactions: the immutans variegation mutant of Arabidopsis is plastid autonomous and impaired in carotenoid biosynthesis. *Plant J*, **6**, 161-175.
- Wright, S.I., Bi, I.V., Schroeder, S.G., Yamasaki, M., Doebley, J.F., McMullen, M.D. and Gaut, B.S. (2005) The effects of artificial selection on the maize genome.

  Science, 308, 1310-1314.
- Wu, D.Y., Wright, D.A., Wetzel, C., Voytas, D.F. and Rodermel, S. (1999) The immutans variegation locus of Arabidopsis defines a mitochondrial alternative oxidase homolog that functions during early chloroplast biogenesis. *Plant Cell*, 11, 43-55.
- Wurtzel, E.T., Cuttriss, A. and Vallabhaneni, R. (2012) Maize provitamin A carotenoids, current resources, and future metabolic engineering challenges.

  Frontiers in Plant Science, 3.
- Yu, F., Fu, A.G., Aluru, M., Park, S., Xu, Y., Liu, H.Y., Liu, X.Y., Foudree, A.,
  Nambogga, M. and Rodermel, S. (2007) Variegation mutants and mechanisms
  of chloroplast biogenesis. *Plant Cell and Environment*, **30**, 350-365.
- Zhou, X.J., Welsch, R., Yang, Y., Alvarez, D., Riediger, M., Yuan, H., Fish, T., Liu,

618	J.P., Thannhauser, T.W. and Li, L. (2015) Arabidopsis OR proteins are the
619	major posttranscriptional regulators of phytoene synthase in controlling
620	carotenoid biosynthesis. Proceedings of the National Academy of Sciences of
621	the United States of America, 112, 3558-3563.
622	
623	

## 624 Figures

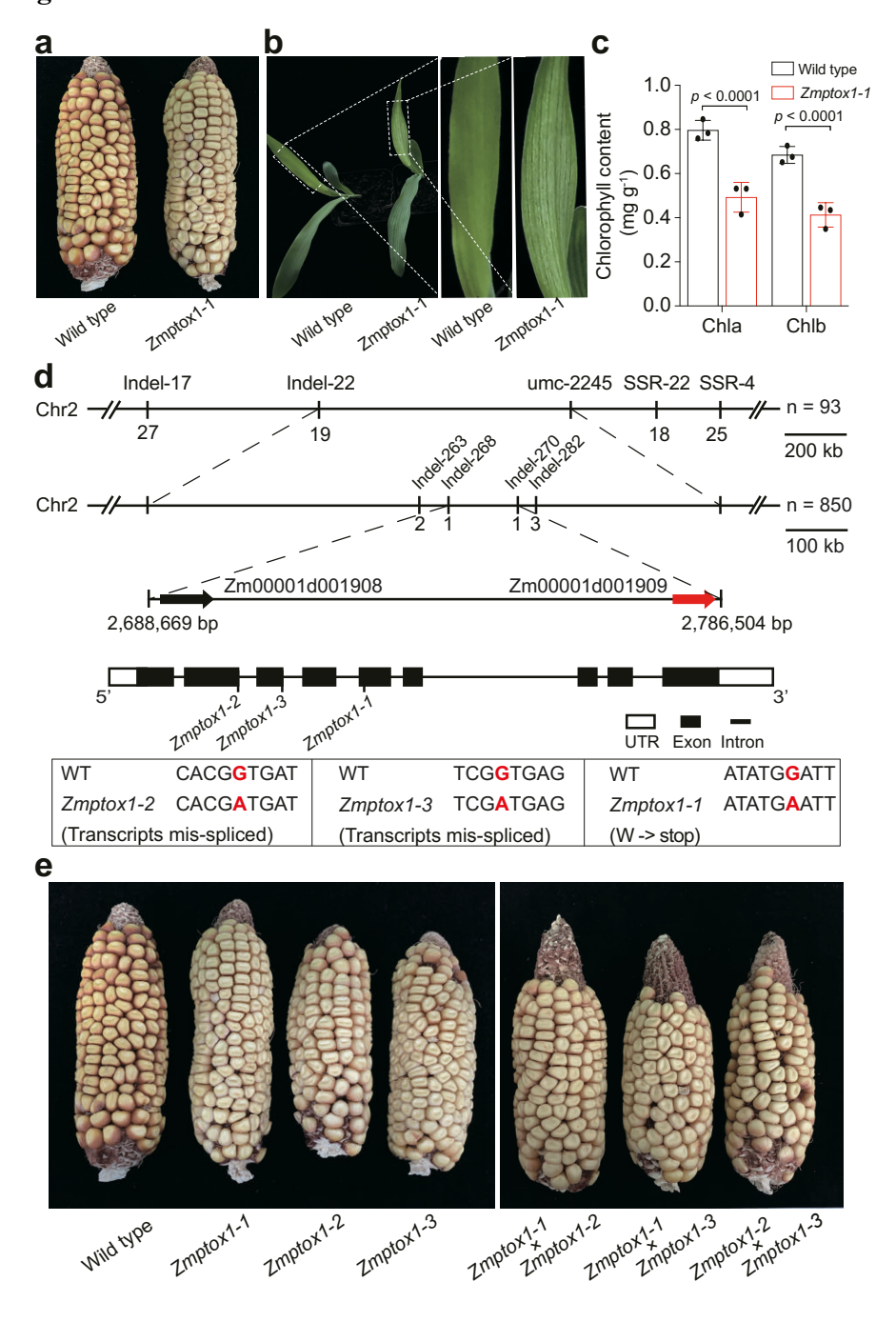


**Figure 1** Map-based cloning of *ZmPTOX1* (a) Ear phenotypes of the wild-type (RP125) and *Zmptox1* mutants. The kernels of mutants are paler than those of the wild type. (b) Leaf phenotype of wild-type and *Zmptox1* mutant plants. The leaves of mutants are paler than those of the wild type. (c) Chlorophyll content of the *Zmptox1* mutant was significantly lower than that of the wild type. (d) Scheme for positional cloning of the *Zmptox1* gene. (e) Comparison of the ear phenotypes of allelic mutants and their progenies with that of the wild type.

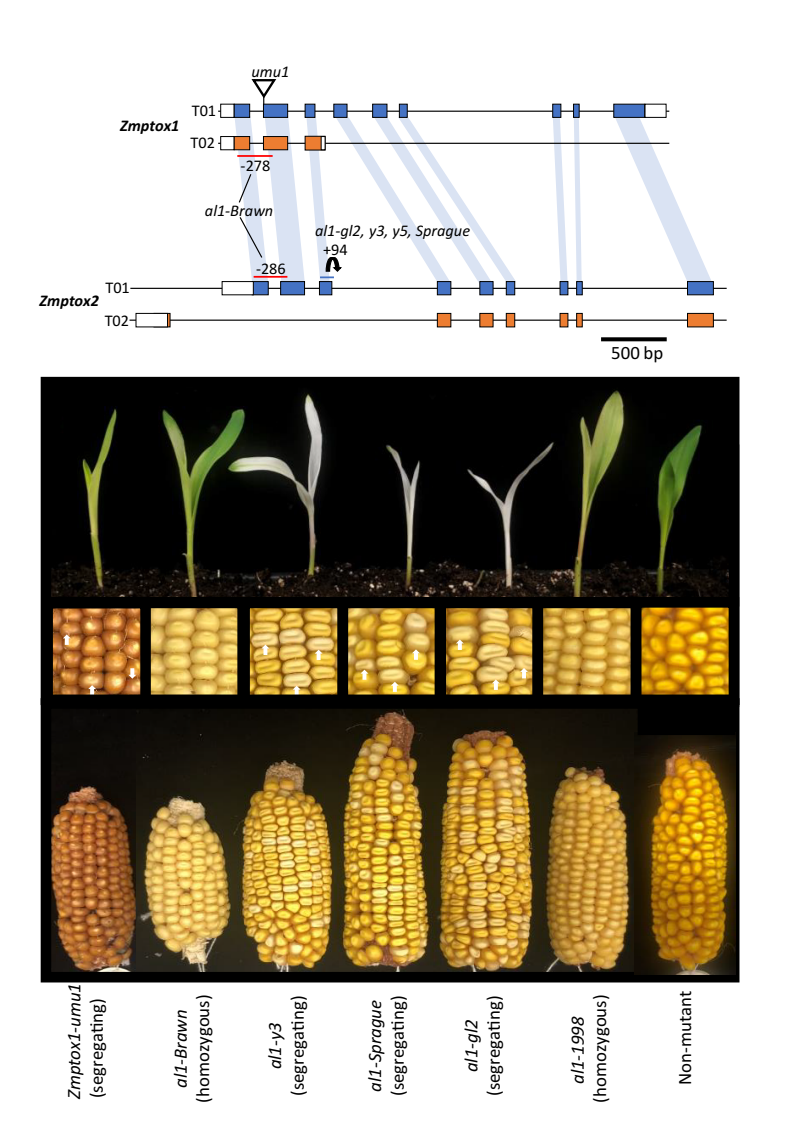
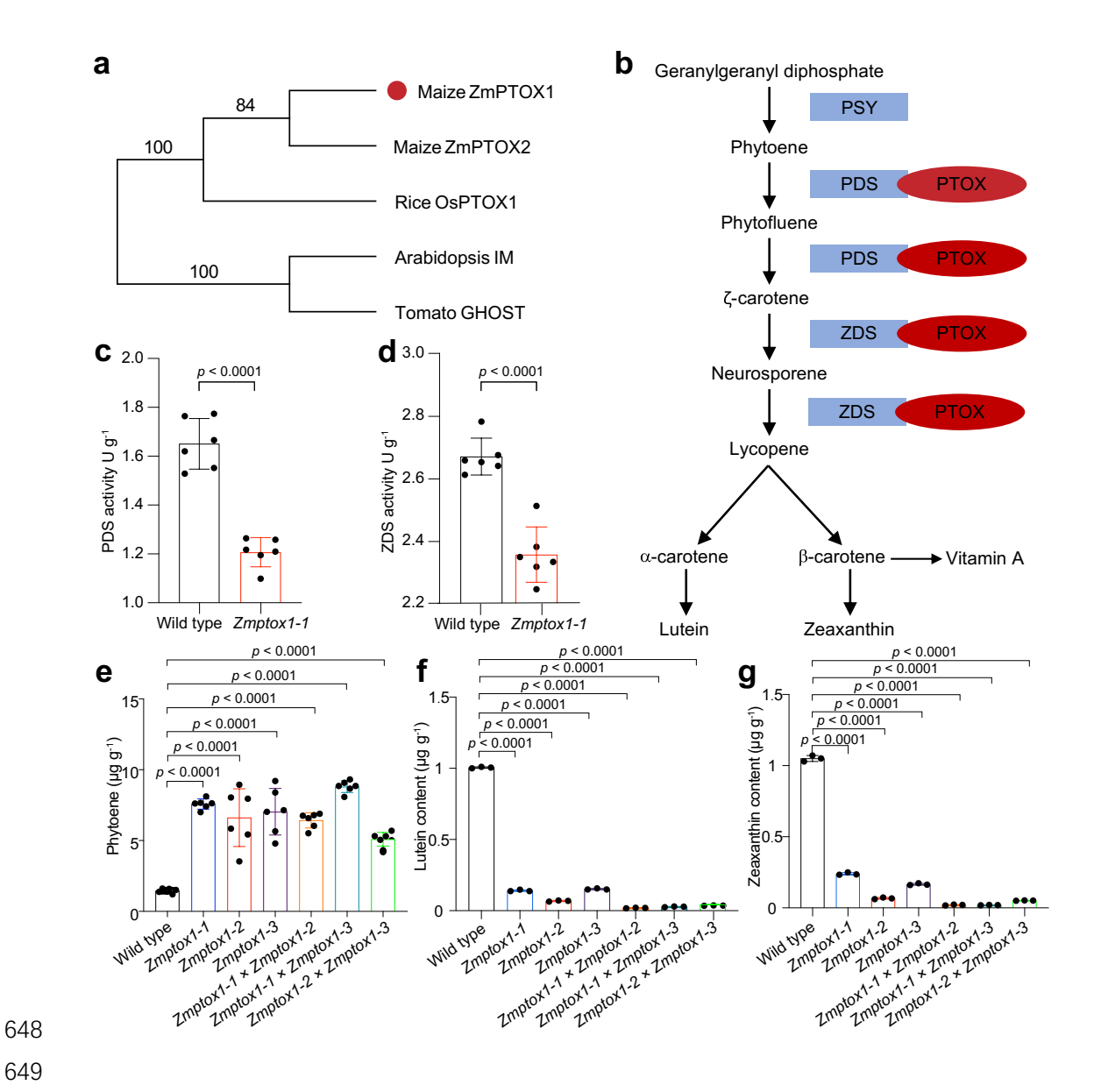
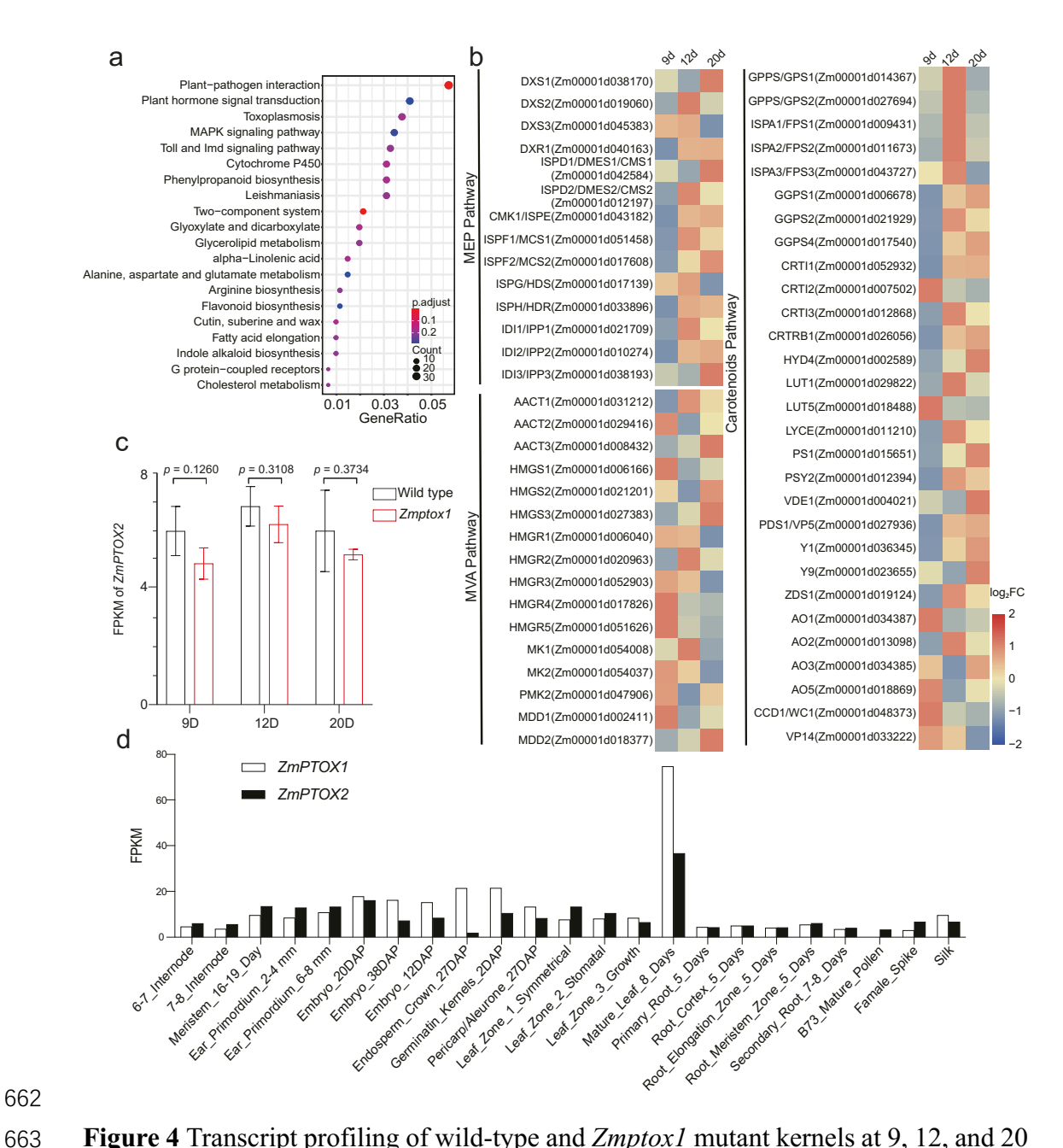


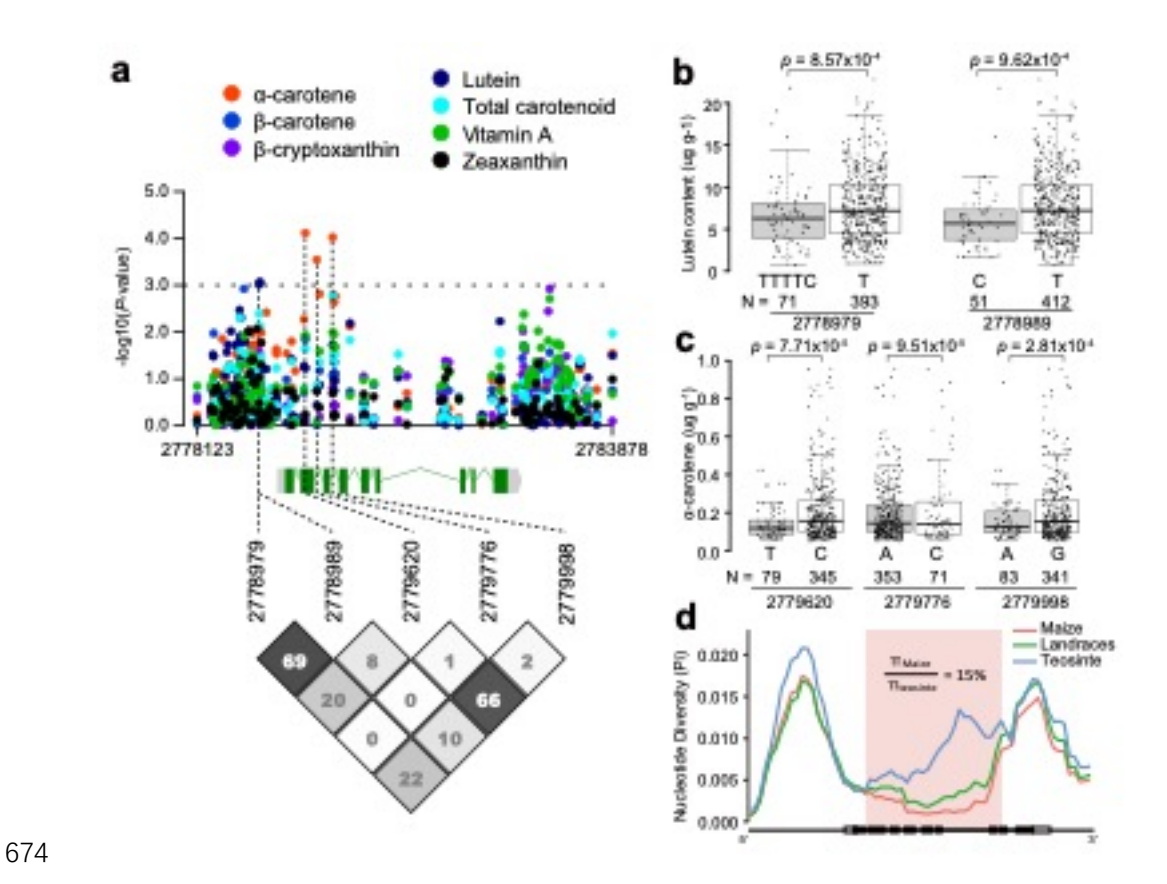
Figure 2 Additional mutations identified in *Zmptox1* and *Zmptox2*. Two UniformMu transposon insertions were identified in *Zmptox1*. The *Zmptox1-umu1* allele at the intron/exon border of the second intron co-segregated with pale kernels that germinated into seedlings with pale leaves. An allelic series of *albescent1* (*al1*) mutants were analyzed for changes to the *Zmptox1* and *Zmptox2* genes. The *al1-Brawn* allele contained similar deletions in both *Zmptox1* and *Zmptox2* resulting in a 62 amino acid in-frame deletion in *Zmptox1* and a frameshift mutation in *Zmptox2*. The *al1-gl2-ref*, *al1-y3*, *al1-y5*, and *al1-Sprague* alleles all contained the same 94-base tandem duplication of exon 3 in *ptox2*. The duplication is retained in the *ZmPTOX2* mRNA and introduces a premature stop codon. This *al1* mutant contains intact, full-length transcript for *Zmptox1*. The *al1-1998* allele did not contain mutations that would be predicted to disrupt translation of either *Zmptox1* or *Zmptox2*.



**Figure 3** *ZmPTOX1* regulates carotenoid biosynthesis in maize kernels. (a) Phylogenetic analysis of *PTOX* genes of maize, rice, Arabidopsis, and tomato. (b) Biosynthetic pathway of lutein and zeaxanthin. (c, d) Activities of PDS (c) and ZDS (d) in *Zmptox1* mutants and wild-type (RP125) plants. (e–g) Contents of phytoene (e), lutein (f), and zeaxanthin (g) in wild-type and *Zmptox1* kernels.



**Figure 4** Transcript profiling of wild-type and *Zmptox1* mutant kernels at 9, 12, and 20 dpp. (a) KEGG enrichment of DEGs. (b) Comparison of the expression levels of MEP, MVP, and carotenoid pathway genes in wild-type controls and *Zmptox1* mutants. (c, d) Expression levels of *ZmPTOX1* and *ZmPTOX2* in mutant and wild-type kernels (c) and other tissues (d).



675676

678

679

680

681

682

683

684

685

686

687

688

689

690

Figure 5 Natural variation in the promoter and open reading frame (ORF) of ZmPTOX1 is associated with the pale color of maize kernels. (a) Two SNPs in the promoter and three SNPs in the ORF of ZmPTOX1 show association with lutein and  $\alpha$ -carotene contents, respectively. The dashed line indicates the threshold of significant association  $(p \le 0.001)$ . The numbers show the pairwise linkage disequilibrium pattern by  $R^2$  (%). The positions of five significant SNPs are shown on the top of the pairwise linkage disequilibrium plot and indicated by dashed lines in the gene diagram. (b, c) The contents of lutein and α-carotene associated with SNPs in diverse inbred lines. Each box represents the median and interquartile range, and whiskers extend to maximum and minimum values. The genotype and number (N) of each allele are listed below each box. (d) Evidence of selection pressure on ZmPTOX1. The red area shows low nucleotide diversity in improved maize lines compared with teosinte, as analyzed using maize HapMap v3 SNP data. Red, green, and blue lines represent the nucleotide diversity of improved maize lines, landraces, and teosinte, respectively. White and black rectangles on the x-axis represent the untranslated regions (UTRs) and exons of the ZmPTOX1 gene.

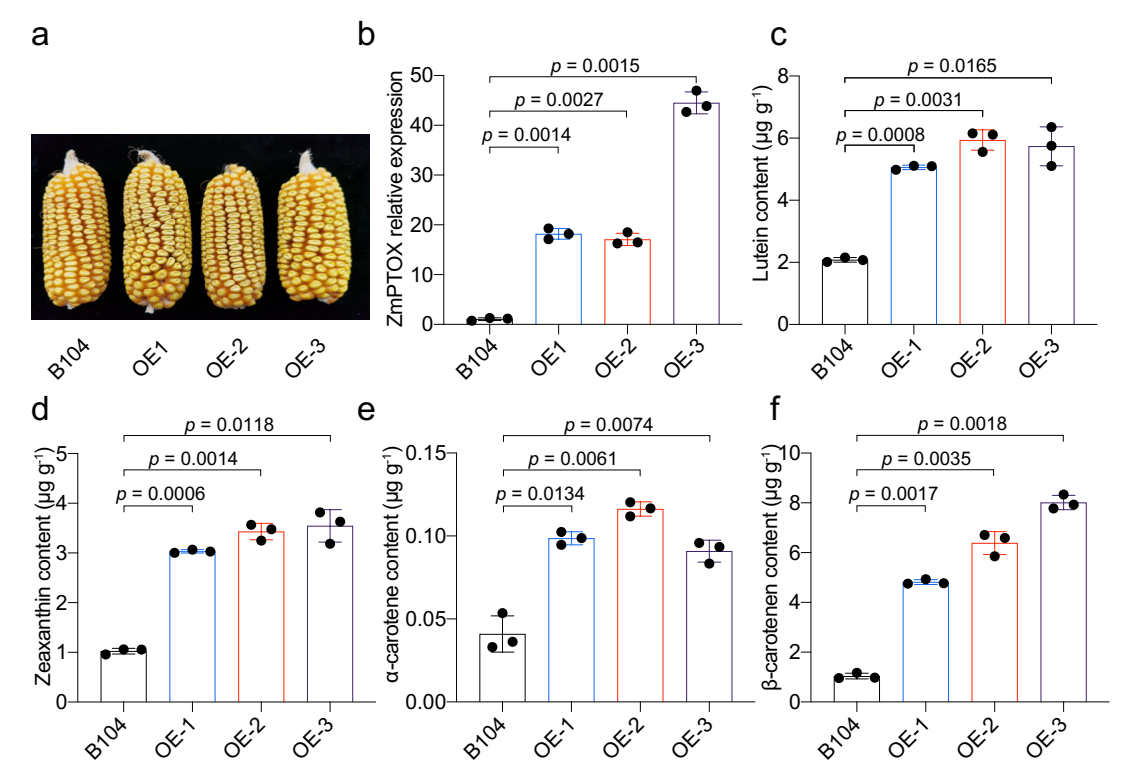


**Figure 6** Characteristics of three Zm*PTOX1*-overexpressing maize lines (OE1–3). (a) Ears of wild-type (B104), OE1, OE2, and OE3 plants. (b) *ZmPTOX1* transcripts were more abundant in the transgenic lines. (c–f) Overexpression of *ZmPTOX1* increased the contents of lutein (c), zeaxanthin (d),  $\alpha$ -carotene (e), and  $\beta$ -carotene (f). In (b–f), data represent mean  $\pm$  standard deviation (SD; n=3). Significant differences were determined using Student's *t*-test. Raw data are plotted in the bar charts.

- Supplementary Figure 1 (a) Comparison of the leaf phenotype of *Zmptox1* mutants
- vith that of the wild type. (b, c, d) Alignment of ZmPTOX1-2, ZmPTOX1-3 and wild
- 715 type alleles.
- 716 **Supplementary Figure 2** Statistics of DEGs. (a) Principal component analysis (PCA)
- of transcriptome data. (b) Venn diagram of upregulated DEGs at 9, 12 and 20d after
- pollination. (c) Venn diagram of downregulated DEGs at 9, 12 and 20d after pollination.
- 719 **Supplementary Figure 3** (a, b) Activities of PDS (a) and ZDS (b) in overexpression
- line and wild-type (B104) plants. (c) The expression of *ZmPSY1* in overexpression
- 721 lines and wild-type (B104) plants.
- 722 **Supplementary Table 1** The list of differentially expressed genes.
- 723 **Supplementary Table 2** The list of primers in this paper.
- 724 **Supplementary Table 3:** The detailed information of *ZmPTOX1* association analysis.
- Supplementary data 1 The full sequences for Zmptox1 and Zmptox2 variants from the
- 726 maize stock center.